ON THE NUMERICAL MODELLING OF SHORT WAVES IN SHALLOW WATER

REPRÉSENTATION, SUR MODÈLE NUMÉRIQUE, DES ONDES DE FAIBLE LONGUEUR SE PROPAGEANT EN EAU PEU PROFONDE

by

M. B. ABBOTT

Reader, International Institute for Hydraulic and Environmental Engineering, Delft, Netherlands,
Head, Computational Hydraulic Centre, Danish Hydraulic Institute, Hørsholm, Denmark

and

H. M. PETERSEN and O. SKOVGAARD

Engineers, Computational Hydraulic Centre, Danish Hydraulic Institute, Hørsholm, Denmark*

Summary A modelling system is described that generates and runs models of short waves of any form (periodic or irregular), with any desired physically realistic current field over any given bathymetry. As this system constitutes the eighth version of the general System 21, "Jupiter", described in an earlier contribution, it is called the "Mark 8". The system-generated models are based upon Boussinesq equations, in which the vertical velocity is supposed to increase linearly from zero at the bed to a maximum magnitude at the surface, in two independent (horizontal) space variables and time. The Boussinesq equations are formulated as mass and momentum conservation laws while, by virtue of the high order of accuracy of the difference approximations, there is very little numerical energy falsification. This formulation also appears to provide genuine weak solutions, for correctly simulating breaking waves, and thus assures the correct simulation of wave thrusts, or radiation stresses, and associated longshore currents.
The System has been tested against analytical results in one and two dimensions and also against physical model tests, for all its main capabilities. In all cases, the agreement of the System model results with the analytical and physical results are satisfactory. The System is already being applied in engineering practice. A discussion is presented of future applications of the System to ship motion simulations, to sediment transport computations and also to more efficient nearly-horizontal flow computations.

Résumé Description d'un système de représentation sur modèle permettant la création et l'exploitation de modèles d'ondes de faible longueur de n'importe quelle forme (périodique ou irrégulière), compte tenu de toute répartition physiquement réaliste des courants sur une répartition bathymétrique donnée quelconque. Du fait que ce Système correspond à la 8ème version du système général 21 "Jupiter" (exposé dans un rapport de publication antérieure), il lui a été affecté la désignation "Mark 8". Les modèles découlant du Système sont établis sur la base des équations de Boussinesq, qui admettent la linéarité de l'accroissement de la vitesse verticale, de la valeur nulle au fond à la valeur maximale au niveau de la surface, en fonction de deux variables spatiales indépendantes (horizontales) et du temps.
Les équations de Boussinesq sont formulées sous la forme de lois de conservation de la masse et de la quantité de mouvement: du fait de l'ordre de précision élevé des approximations de différence, les valeurs numériques de l'energie sont très peu faussées. D'autre part, cette formulation paraît livrer de véritables solutions "faibles" pour la représentation correcte des ondes déferlantes, et par conséquent, pour assurer

* O. Skovgaard now at Lab. Appl. Math. Phys., Tech. Univ. Denmark, Lyngby, Denmark.

Received December 27, 1977 and revised March 11, 1978

la simulation précise des poussées, ou des contraintes de rayonnement et des courants littoraux correspondants, qu'engendrent les ondes considérées.
Les possibilités essentielles du Système présenté ont été vérifiées par confrontation de celui-ci, d'une part à des résultats analytiques uni et bi-dimensionnels, et d'autre part, à des valeurs déterminées sur des modèles réduits. Les résultats déterminés au moyen du modèle du Système s'accordent bien avec les résultats analytiques et du modèle réduit dans tous les cas. Le Système est déja utilisé pour résoudre des problèmes d'hydraulique d'ordre pratique.
En conclusion, les auteurs exposes les différentes possibilités d'extension du Système à des fins telles que la simulation des mouvements des navires, le calcul des débits solides, et d'autre part, en vue d'un meilleur calcul des écoulements quasi-horizontaux.

Introduction

Engineering practice has long been concerned with the behaviour of short-waves in shallow water. For the design of harbours, for example, a detailed knowledge is required of the directions of propagation and the magnitudes of short waves. These waves attack moles, training works and other structures, they infiltrate through harbour entrances to disturb the waters within the harbour area, both directly and through accumulated, seiching actions, they are instrumental in bringing sediments into suspension while they often induce the currents that transport these sediments to quieter regions of deposition, and they may also adversely influence navigation directly. For the control of coastal erosion, as well, a knowledge of short wave motions and the currents that these induce is of fundamental importance, while there are numerous related applications to the design of terminals and other offshore constructions, and to the planning and control of dredging operations.

As a result of the practical interest in these waves, a considerable effort has been made to predict their behaviour along coasts and in and around harbours, terminals and other engineering works. By far the greatest part of this effort has been directed towards developing techniques for physical modelling and a veritable arsenal has been accumulated for this purpose: e.g. field and laboratory instrumentation, wave generators with their associated data-processing, control and evaluation equipment and a wide range of analytical procedures. A particularly significant development has been the introduction of irregular wave generators, whereby a local wave climate can be established that is far more realistic for most applications than that obtained with periodic waves [e.g. SORENSEN, 1973].

The effort expended in numerical modelling, although considerably less than that used in physical modelling, has still produced several useful techniques. Most of these techniques are based upon analogies between periodic wave propagation and the propagation of light waves, whereby advanced methods of geometric optics can be carried over to the study of the behaviour of periodic water waves. However, the range of water waves that can be so treated is very restricted, being essentially limited to small-amplitude periodic waves, described by linearised wave theories, as outlined in more detail below. Although the behaviour of these waves may often provide some guide to real wave behaviour, the experience of physical modelling suggests that the restrictions of small amplitude and periodicity, so the restrictions essential to the linearised theory, give unacceptable errors in many practical situations. Thus, if numerical simulation is to meet the needs of practice, even if only going so far as is possible with physical simulations, so as to interact with these simulations, numerical methods have to be introduced that are not subject to the linearising restrictions. The present paper describes such methods and shows how they are capable of providing comparable information to that obtainable from physical modelling, so as to be compatible with physical modelling techniques, thus improving the overall reliability of the engineering investigation and design process.

Review of background material

In order to relate the present work and the methods that it proposes to earlier works and their methods, and to provide a basis for some comparisons, a rather extensive review of theories and methodologies is necessary. This review encompasses the four main streams of development that have influenced the present work, namely (1) the analysis of alternative differential formulations, (2) analyses of numerical formulations, (3) recent work on the orders of approximation implicit in differential formulations and the consequences of this work for the numerical formulations and (4) the development and refinement of modelling systems for nearly-horizontal flows. These are considered in order, as follows:

(1) The terminology of "short" waves is that of common engineering practice. In classical hydrodynamics, however, what are here called "short" shallow water waves are viewed as waves whose length is still large compared with the depth of the water in which they propagate and they are, correspondingly, usually subsumed under "long waves". The various theories constructed to describe the behaviour of these waves are generally characterized by an URSELL number:

$$U_* = \frac{\zeta_* L_*^2}{h_*^3}$$

where ζ_* is a measure of the wave amplitude, L_* is a characteristic horizontal length of the surface profile and h_* is a measure of the water depth [URSELL, 1953]. The earliest relevant theory, of

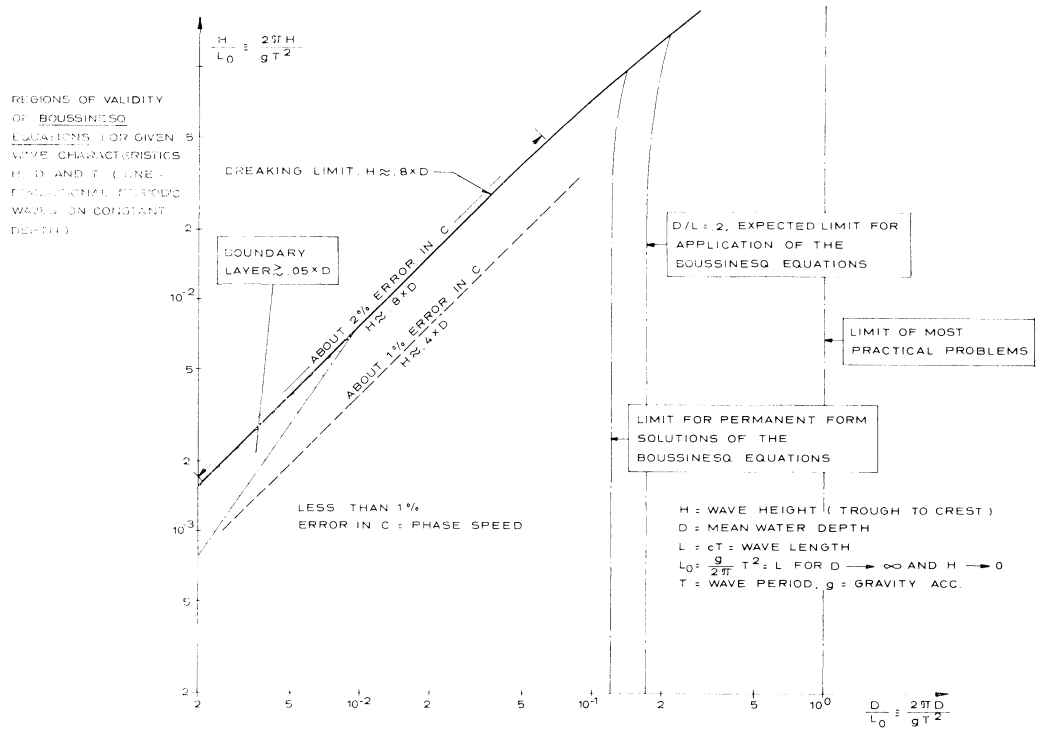

a. Range of application of the mass and BOUSSINESQ equation system (4, 5, 6).

Fig. 1.

a. Domaine de validité du système des équations de masse et de BOUSSINESQ (4, 5, 6).

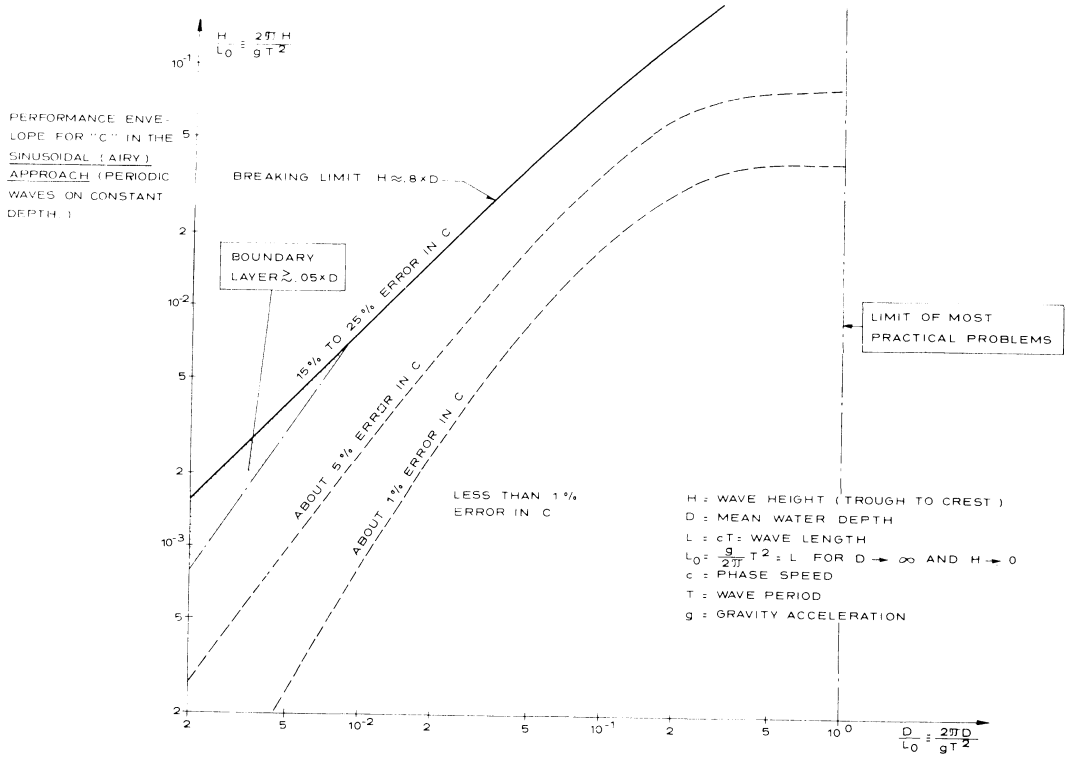

b. The corresponding range of application of the sinusoidal wave approximation.

Fig. 1.

b. Domaine de validité correspondant de l'approximation d'onde sinusoïdale.

AIRY [1845], makes the assumption that the pressure distribution in the vertical is hydrostatic. The resulting waves are non-dispersive, while waves of finite amplitude cannot propagate without change of shape. AIRY's theory corresponds to $U_* \gg 0(1)$. The symmetric case of $U_* \ll 0(1)$ is covered by the linearised shallow water theory of JEFFREYS and JEFFREYS [1946], which also assumes a hydrostatic pressure distribution.

Between the theories of AIRY and JEFFREYS and JEFFREYS there is the theory of BOUSSINESQ [1872, 1877]. In this theory the curvature of streamlines in the vertical plane is described through a vertical velocity the magnitude of which increases linearly from zero at the bed to a maximum at the free surface. In this theory, therefore, the pressure distribution is no longer hydrostatic, but the vertical component of motion can be integrated out of the equations of motion to reduce the three dimensional description to a two-dimensional one. The original theory held for the irrotational motion of an incompressible, homogeneous, inviscid fluid over a horizontal bed, while only solutions for uni-directional wave propagation were considered. URSELL [1953] showed that the BOUSSINESQ theory included the AIRY and JEFFREYS and JEFFREYS theories as special cases. As shown later (e.g. Fig. 1), the BOUSSINESQ theory may in fact be regarded as the most uniformly valid basis for finite amplitude water waves so long as h_*/L_* remains small and breaking does not occur.

When $U_* = 0(1)$ the non-linear, governing equations for a horizontal bottom are of the KORTEWEG-DE VRIES [1895] type, that have unidirectional cnoidal waves as permanent solutions. LIN and CLARK [1959] extended solutions of the BOUSSINESQ theory to include diffracted and reflected

plane waves over a horizontal bed while MEI and LE MÉHAUTÉ [1966] extended the theory to account for a slowly varying bathymetry [see also MADSEN and MEI, 1969]. In 1967, PEREGRINE derived the BOUSSINESQ-type equations governing the propagation of arbitrary, long-wave disturbances of small to moderate amplitude over a slowly-varying bathymetry. His equations read

$$\frac{\partial \zeta}{\partial t} + \frac{\partial}{\partial x}[(D+\zeta)u] + \frac{\partial}{\partial y}[(D+\zeta)v] = 0 \tag{1}$$

$$\frac{\partial u}{\partial t} + u\frac{\partial u}{\partial x} + v\frac{\partial u}{\partial y} + g\frac{\partial \zeta}{\partial x} = \tfrac{1}{2}D\left[\frac{\partial^3(Du)}{\partial x^2 \partial t} + \frac{\partial^3(Dv)}{\partial x \partial y \partial t}\right] - \tfrac{1}{6}D^2\left[\frac{\partial^3 u}{\partial x^2 \partial t} + \frac{\partial^3 v}{\partial x \partial y \partial t}\right] \tag{2}$$

$$\frac{\partial v}{\partial t} + u\frac{\partial v}{\partial x} + v\frac{\partial v}{\partial y} + g\frac{\partial \zeta}{\partial y} = \tfrac{1}{2}D\left[\frac{\partial^3(Dv)}{\partial y^2 \partial t} + \frac{\partial^3(Du)}{\partial x \partial y \partial t}\right] - \tfrac{1}{6}D^2\left[\frac{\partial^3 v}{\partial y^2 \partial t} + \frac{\partial^3 u}{\partial x \partial y \partial t}\right] \tag{3}$$

where $z = -D(x,y)$ corresponds to the bed elevation. In terms of depth-integrated velocities, which are alternatively volume flux densities or horizontal-momentum levels divided by the (specific mass) density, these governing equations become,

$$\frac{\partial \zeta}{\partial t} + \frac{\partial p}{\partial x} + \frac{\partial q}{\partial y} = 0 \tag{4}$$

$$\frac{\partial p}{\partial t} + \frac{\partial}{\partial x}\left(\frac{p^2}{h}\right) + \frac{\partial}{\partial y}\left(\frac{pq}{h}\right) + gh\frac{\partial \zeta}{\partial x} = \tfrac{1}{2}Dh\left[\frac{\partial^3}{\partial x^2 \partial t}\left(\frac{Dp}{h}\right) + \frac{\partial^3}{\partial x \partial y \partial t}\left(\frac{Dq}{h}\right)\right] - \tfrac{1}{6}D^2 h\left[\frac{\partial^3}{\partial x^2 \partial t}\left(\frac{p}{h}\right) + \frac{\partial^3}{\partial x \partial y \partial t}\left(\frac{q}{h}\right)\right] \tag{5}$$

$$\frac{\partial q}{\partial t} + \frac{\partial}{\partial y}\left(\frac{q^2}{h}\right) + \frac{\partial}{\partial x}\left(\frac{pq}{h}\right) + gh\frac{\partial \zeta}{\partial y} = \tfrac{1}{2}Dh\left[\frac{\partial^3}{\partial y^2 \partial t}\left(\frac{Dq}{h}\right) + \frac{\partial^3}{\partial x \partial y \partial t}\left(\frac{Dp}{h}\right)\right] - \tfrac{1}{6}D^2 h\left[\frac{\partial^3}{\partial y^2 \partial t}\left(\frac{q}{h}\right) + \frac{\partial^3}{\partial x \partial y \partial t}\left(\frac{p}{h}\right)\right] \tag{6}$$

where $h \equiv D + \zeta$, $p = uh$ and $q = vh$. It is equations (4, 5, 6), augmented with other terms, such as those that account for a reduced flow area (permeable breakwater) and corresponding resistance terms (equations 11, 12, 13), and also wave resistance terms, that are solved by the present System. As described in detail later, equations (4, 5, 6) do not have a unique form, but can be rewritten by using relations corresponding to equations of lower order. The range of applications of equations (4, 5, 6) is shown in fig. 1a. This figure is based upon a comparison between one-dimensional Cnoidal-wave solutions of (4, 5, 6) and the permanent wave solutions of DEAN (1974].

The theory constituted by equations (4, 5, 6) with their corresponding classes of solution functions evidently includes sub-theories corresponding to simpler linearised equations, such as those corresponding to the classical linearized long wave equations for periodic waves of small amplitude ($U_* \ll 0(1)$):

$$\frac{\partial}{\partial x}\left(D\frac{\partial \zeta^*}{\partial x}\right) + \frac{\partial}{\partial y}\left(D\frac{\partial \zeta^*}{\partial y}\right) + Dk^2\zeta^* = 0 \tag{7}$$

In (7) $\zeta^* = \zeta^*(x,y)$ is a complex wave amplitude so that $\zeta^* \exp(-i\omega t)$ is the instantaneous elevation of the water surface, ω is the angular frequency and k is the wave number. Equation (7) can also be regarded as a special non-dispersive version of BERKHOFF's [1973, 1976] wave equation for intermediate depths and mild slopes [see also JONSSON et al, 1976]:

$$\frac{\partial}{\partial x}\left(cc_g \frac{\partial \zeta^*}{\partial x}\right) + \frac{\partial}{\partial y}\left(cc_g \frac{\partial \zeta^*}{\partial y}\right) + cc_g k^2 \zeta^* = 0 \tag{8}$$

where c and c_g are the phase and group celerities respectively of classical small-amplitude sinusoidal wave theory. BERKHOFF's [1976] linear wave equation also assumes periodic waves with $U_* \ll 0(1)$ but it is not restricted to hydrodynamically "long" waves. By virtue of the linearisation, arbitrary input waves can also be built up from Fourier components in BERKHOFF's theory and their solutions obtained by superimposing the corresponding component solutions, but this leads to considerable complication over and above the restrictive conditions. The use of the linear long wave equation appears to be implicit in the solution method of CHEN and MEI [1974, 1976] while the use of this equation or BERKHOFF's linear equation appears to be implicit in the methods of ZIENKIEWICZ and BETTESS [1976] and BETTESS and BETTESS [1976].

BERKHOFF's wave equation describes combined diffraction-refraction, but if reflections can be ignored it is possible to reduce this equation so as to address depth refraction only, without diffraction, reflection or scattering. This equation then provides the well-known eiconal equation of geometric optics [e.g. BORN and WOLF, 1975. See also BERKHOFF, 1976].

The extension of the solution of the general equations (4, 5, 6) to allow for wave breaking, by the introduction of a suitable (non-linear) dissipative interface [ABBOTT, 1974] allows the simultaneous computation of wave-induced currents [LONGUET HIGGINS and STEWART, 1960, 1962; LUNDGREN, 1963], and thence a rational approach to sediment transport within the breaker zone [e.g. JONSSON et al, 1975]. This use of the present code involves so much other material, however, that it can best form the subject of a separate communication. Similarly, the computation of ship motions simultaneously with short-period wave motions, already realised with the present method, will be treated in a separate communication.

(2) The second point of departure for the present work was the numerical solution of Boussinesq-type equations by RODENHUIS [1966], described with a summary of earlier work by ABBOTT and RODENHUIS [1972]. This work showed the extreme sensitivity of the solutions of the equations to numerical error influences and the necessity, for practical applications, of a high-accuracy difference scheme. It also indicated, however, that an excellent agreement could be obtained between solutions of difference forms of the Boussinesq equations and real-world finite amplitude waves if sufficient numerical accuracy could be obtained.

(3) The third point of departure was the systematic study, in mathematical fluid mechanics, of the orders of approximation implicit in differential formulations of the present problem. The development of this study can be traced through the papers of FRIEDRICHS [1948], STOKER [1955], LONG [1964], RODENHUIS [1966], MEYER [1967], PEREGRINE [1967, 1972, 1974], BENJAMIN, BONA and MAHONY [1972] and BONA and SMITH [1976]. The most significant result of this development, from the present point of view, was the observation [originally, it seems, of LONG, 1964] that the higher-order terms of BOUSSINESQ-type equations could be rewritten by using the linearized wave equations

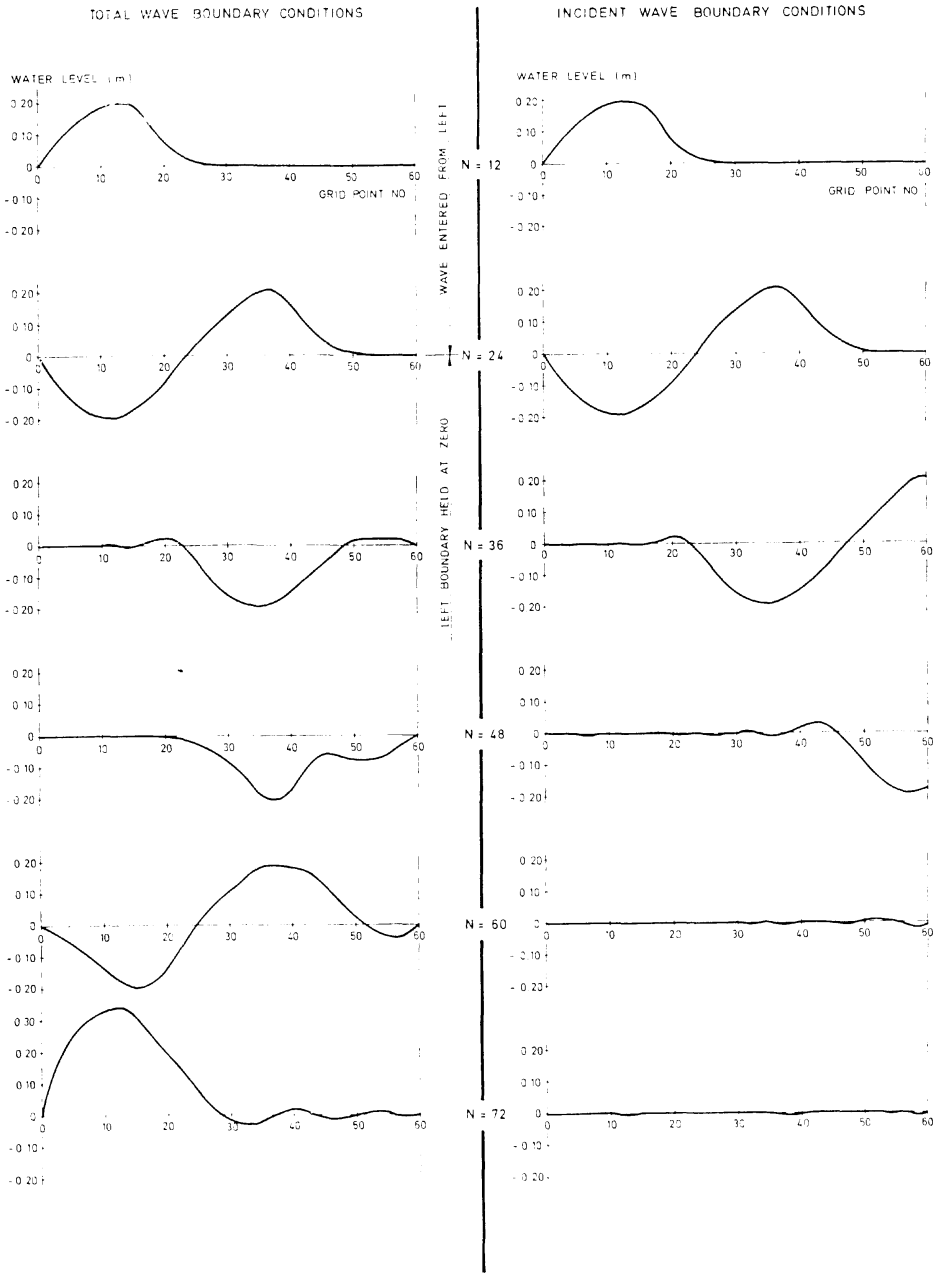

Rig test of the wave-filtering boundary module, or SOMMERFELD boundary module, showing how:

a. As opposed to allowing a wave to be totally reflected (left) it allows it to be totally absorbed (right).

Fig. 2a.

Essais en laboratoire du module filtre-d'onde pariétal (ou module pariétal de SOMMERFELD), mettant en évidence:

a. Comment il permet à une vague d'être completement amortie (droite) ou au contraire d'être completement réfléchie (gauche).

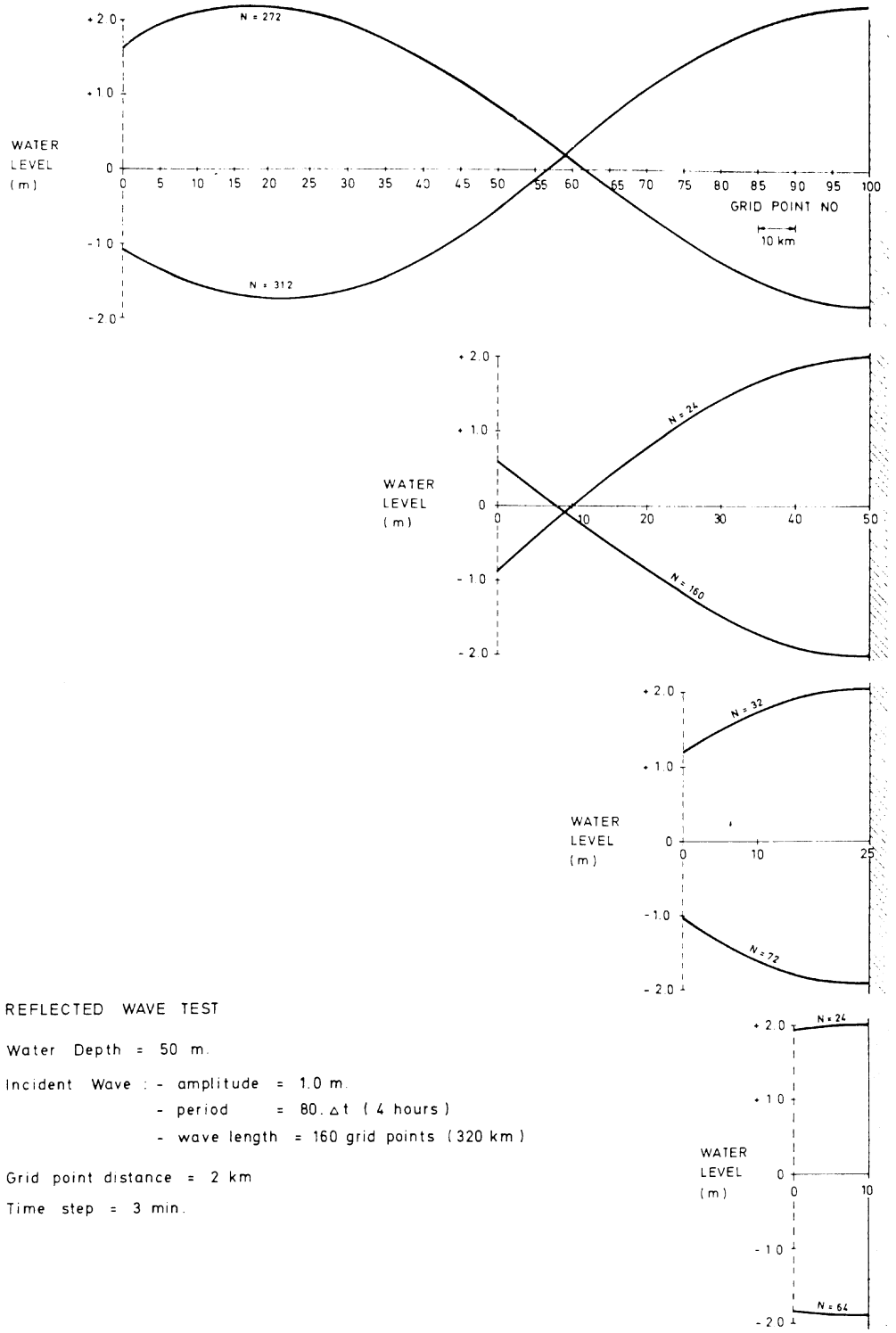

REFLECTED WAVE TEST

Water Depth = 50 m.

Incident Wave : - amplitude = 1.0 m.
- period = 80. Δt (4 hours)
- wave length = 160 grid points (320 km)

Grid point distance = 2 km

Time step = 3 min.

Fig. 2b.

b. It enables the model to be cut at any point and the solution to be generated on one side of the cut and

b. la possibilité de couper le modèle en tout point, et d'élaborer la solution d'un côté de la coupure,

$$\frac{\partial u}{\partial t} + g\frac{\partial \zeta}{\partial x} = 0 \tag{9}$$

$$\frac{\partial \zeta}{\partial t} + D\frac{\partial u}{\partial x} = 0 \tag{10}$$

without any loss of generality or accuracy. The parallel study of consistency of difference schemes then suggested that the same, much simplified substitution could be used at the level of the difference equations, so as to transform the high-accuracy but algorithmically intractable difference forms of the Boussinesq equations (4, 5, 6) into algorithmically efficient difference schemes, as exemplified in Appendix 1.

(4) The fourth development that was of decisive importance for the present work was the construction and refinement of the modelling system for nearly-horizontal flows, System 21, "Jupiter" [e.g. ABBOTT, DAMSGAARD and RODENHUIS, 1973; ABBOTT, 1976, 1, 2, 3]. For reasons quite

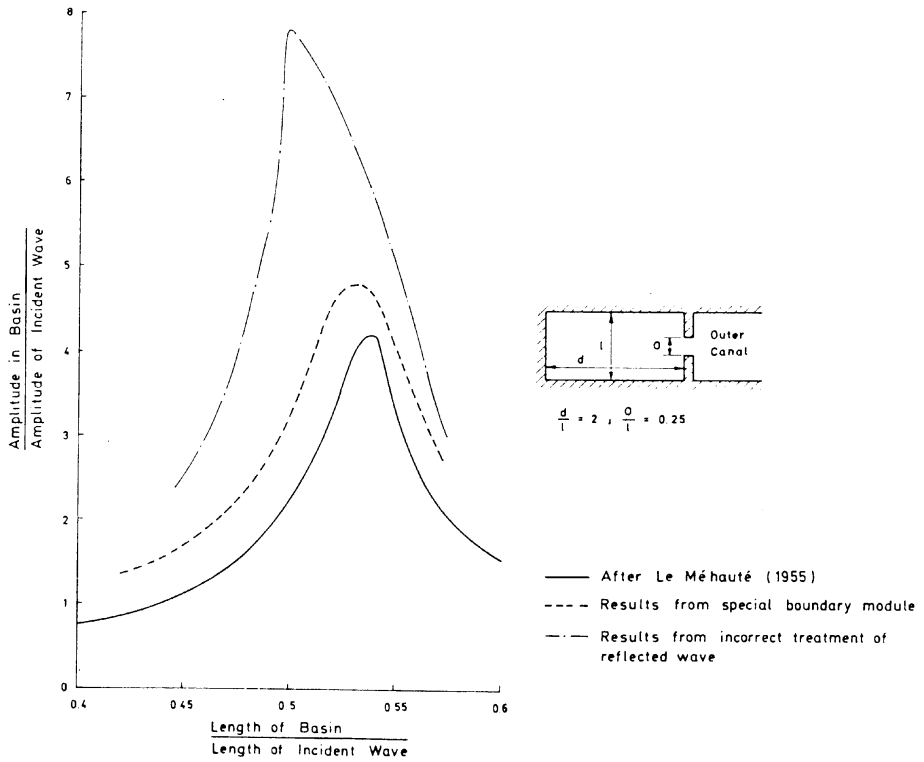

Fig. 2c.

c. how the use of the module at the harbour entrance provides a better comparison with analysis and experiments in a harbour subject to nearly-horizontal flow seiching, as compared to the use of raw elevation data at the harbour entrance.

c. comment l'utilisation de module à l'entrée du port permet une meilleure confrontation des résultats à ceux déterminés par analyse ou sur modèle réduit, pour le cas d'un port affecté de balancements du type seiche de l'écoulement dans le sens quasi-horizontal, que si l'on ne tenait compte que des cotes d'altitude brutes à l'entrée du port.

unconnected with the present work, this had been brought to third-order accuracy in its convective components so that a relatively minor effort was required to bring its other mass-conservation and impulse-momentum components, both differentials and their coefficients, to the required level of accuracy, using the elimination techniques of the type described in Appendix 1. Moreover, the system speed and reliability had been increased to such an extent that it appeared that the new short-wave variant, even though necessarily working with a fine mesh, could still provide a useful instrument for engineering practice. In particular, the existing variant was both non-linearly and linearly stable for all physically possible boundary conditions [DAUBERT and GRAFFE, 1967], and these properties carried over to the new variant.

Among the many existing support and service programs that were carried over to the new variant, the most important was a filtering boundary module, that allowed the filtering-out of incoming wave trains from outgoing wave trains in any wave record, using a System-built model of the wave-recording situation. This then allowed models of water bodies containing post-measurement constructions to be cut out along any convenient line, with the incoming wave trains being maintained as measured and the new reflected wave trains being passed-out through the boundary. Two of the many test-rig trials of this filtering module are illustrated in Fig. 2. Among other applications, this module makes possible the maintenance of a steady realistic sea state within any region regardless of the objects (harbours, ships, terminals, platforms etc.) placed within that region. Since the first formulation of such a boundary condition was given by SOMMERFELD (1964), this module is called the "SOMMERFELD boundary module".

Further formulations

The differential equations solved in open water regions have already been given as (4, 5, 6) above. In the case that the flow area is restricted, as occurs especially at permeable breakwaters, these equations generalise to

$$n\frac{\partial \zeta}{\partial t} + \frac{\partial p}{\partial x} + \frac{\partial q}{\partial y} = 0 \tag{11}$$

$$n\frac{\partial p}{\partial t} + \frac{\partial}{\partial x}\left(\frac{p^2}{h}\right) + \frac{\partial}{\partial y}\left(\frac{pq}{h}\right) + gh\frac{\partial \zeta}{\partial x}n^2 + \frac{nhz}{3}\frac{\partial^3 p}{\partial x^2 \partial t} + \frac{nhz}{3}\frac{\partial^3 q}{\partial x \partial y \partial t} +$$
$$+(1-n)^3\frac{\alpha v}{d^2}p + \frac{(1-n)}{n}\frac{\beta}{d}\cdot p\sqrt{\left(\frac{p}{h}\right)^2 + \left(\frac{q}{h}\right)^2} = 0 \tag{12}$$

$$n\frac{\partial q}{\partial t} + \frac{\partial}{\partial y}\left(\frac{q^2}{h}\right) + \frac{\partial}{\partial x}\left(\frac{pq}{h}\right) + gh\frac{\partial \zeta}{\partial y}n^2 + \frac{nhz}{3}\frac{\partial^3 q}{\partial y^2 \partial t} + \frac{nhz}{3}\frac{\partial^3 p}{\partial x \partial y \partial t} +$$
$$+(1-n)^3\frac{\alpha v}{d^2}q + \frac{(1-n)}{n}\frac{\beta}{d}\cdot q\sqrt{\left(\frac{p}{h}\right)^2 + \left(\frac{q}{h}\right)^2} = 0 \tag{13}$$

with n the pore volume. (Here z is held constant for simplicity of exposition.)

The laminar-flow resistance term is introduced in order to provide realistic simulations of reduced-scale, physical model tests. The equations are further augmented by wave resistance terms of the type developed by JONSSON [1967]. Conservations forms and distributional formula-

tions are further necessary when treating breaking waves for wave-induced currents [WHITHAM, 1974; ABBOTT, 1974].

The construction of a high-accuracy (at least third-order accurate) difference approximation to (4, 5, 6) or its generalisation (11, 12, 13), necessitates the use of a four-stage difference scheme with memory components [ABBOTT, 1978]. The principle of the technique used is described in the Appendix for a one-dimensional descent based upon the implicit scheme of PREISSMANN [LIGGETT and CUNGE, 1975]. In this case, which is probably the simplest of all, it is seen how the zero-order equation system (9, 10) is used to provide a scheme that requires only one time level of memory more than is required by the nearly-horizontal flow system and which remains very fast in operation.

Performance envelope testing

A range of descriptive parameters within which a system provides usable results, together with error estimates over this range, consistutes a "performance envelope" for the system. The envelope for the differential basis of the Mark 8 has been described in Fig. 1a, while Fig. 1b provides an envelope for the differential basis of models restricted to the linear-approximation. The envelope for the difference scheme approximation is usually more restricted than is the envelope of the differential forms themselves, because of the errors inherent in numerical approximations, while correspondingly it contains additional numerical parameters over and above the physical parameters of the differential form. The objective here was to extend the envelope of the difference form to fill-out so far as possible the envelope of the differential form, schematized in Fig. 1a.

In view of the marked non-linearity of the Boussinesq equations, which must carry over to their numerical approximations, the definition of the performance envelope necessitated a very extensive program of testing.

The tests were conducted in terms of the dimensionless dependent variables:

$$P = \frac{\text{amplitude of waves generated by the difference equations}}{\text{amplitude of waves generated by the differential equations}}, \tag{14}$$

a measure of the amplification error, and

$$Q = \frac{\text{celerity of waves generated by the difference equations}}{\text{celerity of waves generated by the differential equations}}, \tag{15}$$

a measure of the phase error

where the waves generated by the differential equations are cnoidal waves in all performance envelope test cases. The dimensionless independent variables were:

$$R = \frac{\text{wave amplitude}}{\text{still water depth}} \tag{16}$$

$$S = \frac{\text{wave length}}{\text{still water depth}} \tag{17}$$

augmented by the numerical parameters

$$Cr = c_{\pm}\left(\frac{\Delta t}{\Delta x}\right) \tag{18}$$

with $c_{\pm}$ the dynamic wave celerities generated by the differential equations (4, 5, 6) or equivalently (11, 12, 13) and

$$N_x = \frac{2l}{k\Delta x}, \qquad N_t = \frac{N_x}{Cr} \tag{19}$$

the number of computational points per wave length in space and time respectively, at dimensionless wave number k.

Fig. 3a shows a test at a low ratio of wave amplitude to wave length, R, and low Courant number, Cr, in which a very small number of points per wave length ($N_x = 8$ to 12) are seen to be sufficient to provide $P \approx 1$ and $Q \approx 1$. Fig. 3b shows how, as the ratio of wave amplitude to wave length increases, so a significant phase error, measured by Q, appears, even for N_x, $\approx N_t$, $= 11$. Increasing N_x, $\approx N_t$, to 22 removes the phase error in this case, as shown in Fig. 3c. This test illustrates the interaction between physical and numerical parameters in the performance envelope, corresponding to the marked non-linearity of the governing equations.

Two schematizations of the performance envelope for uni-directional propagation, based on some 120 test runs, are shown in Fig. 4. It is seen that, for $Cr \approx 1$, an acceptable accuracy is obtained with values of $N_x(\approx N_t)$ as low as 6.

Since much the greater part of the energy of irregular waves is usually distributed over wave

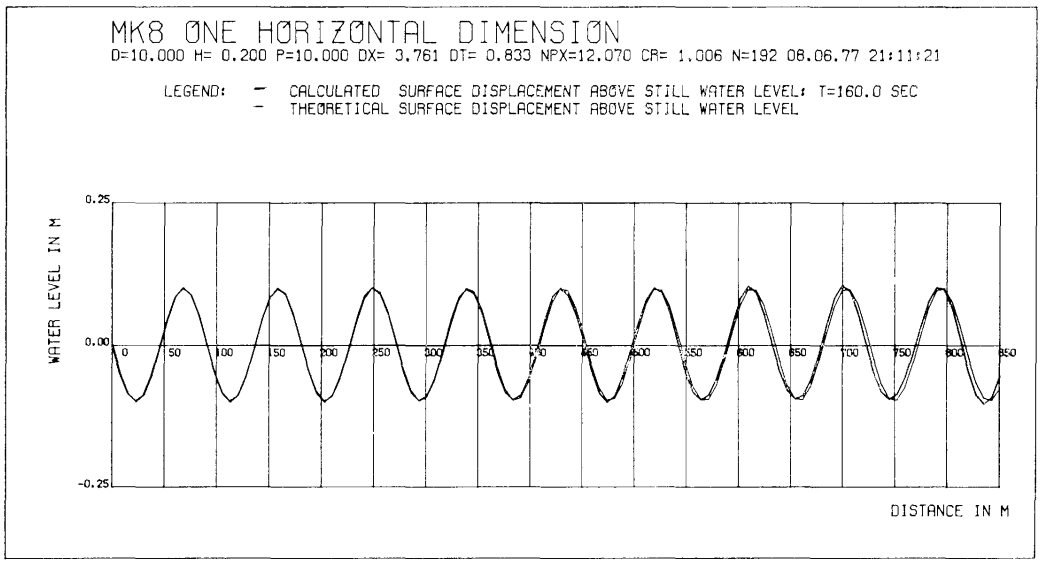

a. Comparison between a numerically computed wave train and the corresponding analytical (Cnoidal) wave train at $Fr \approx 1$ for a low ratio of wave amplitude to wave length but small N_x.

Fig. 3.

a. Confrontation d'un train d'ondes, déterminé par le calcul, au train analytique (cnoïdal) correspondant, avec $Fr \approx 1$ et une faible valeur du rapport de l'amplitude par la longeur de l'onde, mais aussi de N_x.

component periods greater than 4 seconds, at least for the applications envisaged for the present system, Fig. 4 indicates that time steps of about 1 second can be used in many practical situations, giving distance steps of the order of 10 m. These parameters are such as to assure the viability of the system in engineering practice.

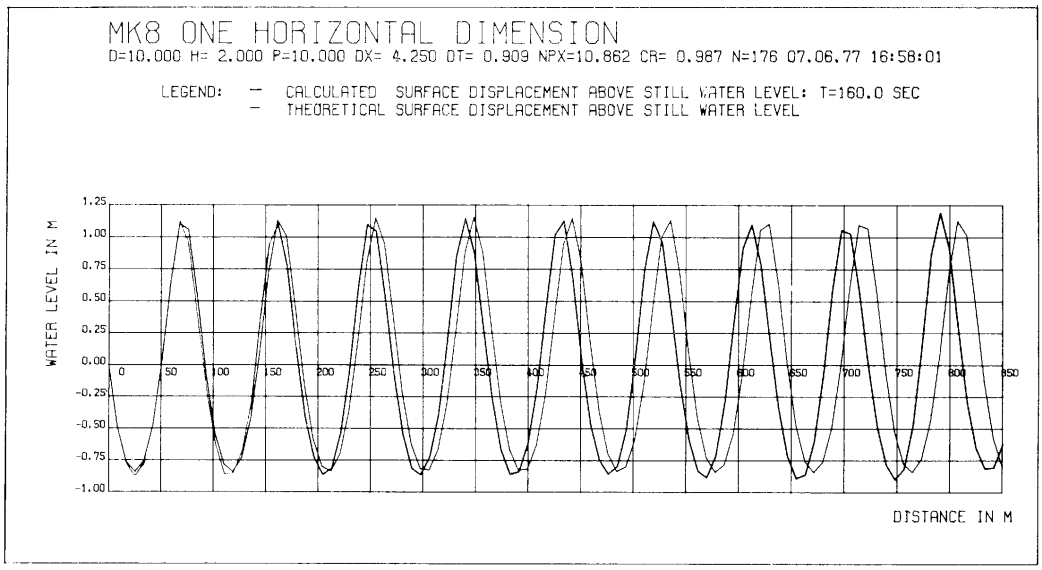

b. The comparison taken at a considerably higher ratio of wave amplitude to wave length, showing how a phase error appears even at $N_x(\approx N_t) = 11$.

b. Cette même confrontation, mais compte tenu d'un valeur très nettement plus élevée du rapport amplitude/longueur, mettant en évidence l'apparition d'un déphasage, même avec $N_x(\approx N_t) = 11$.

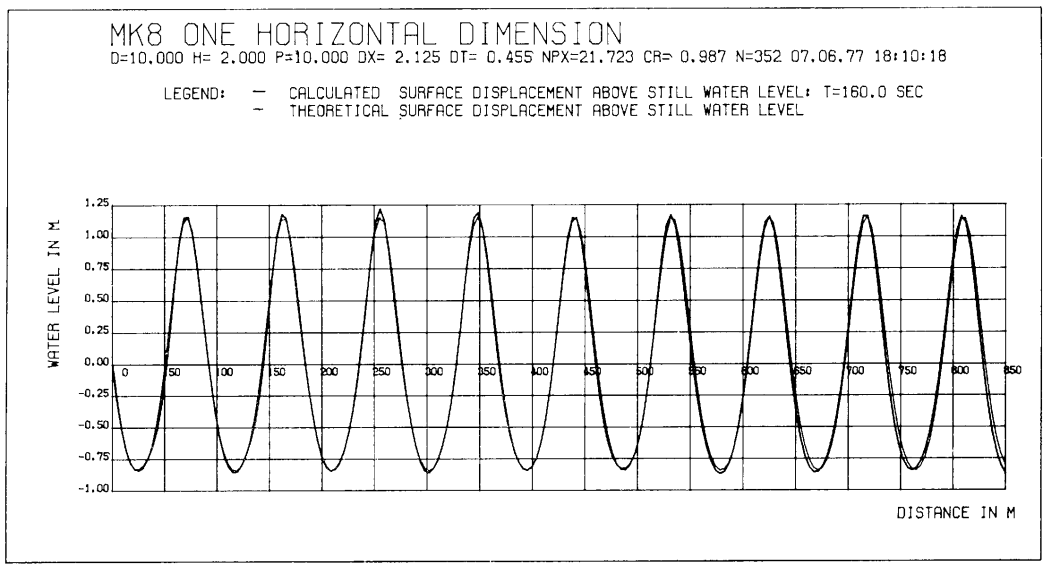

c. When $N_x(\approx N_t) = 22$, this phase error disappears again.

c. Ce déphasage disparaît de nouveau si $N_x(\approx N_t) = 22$.

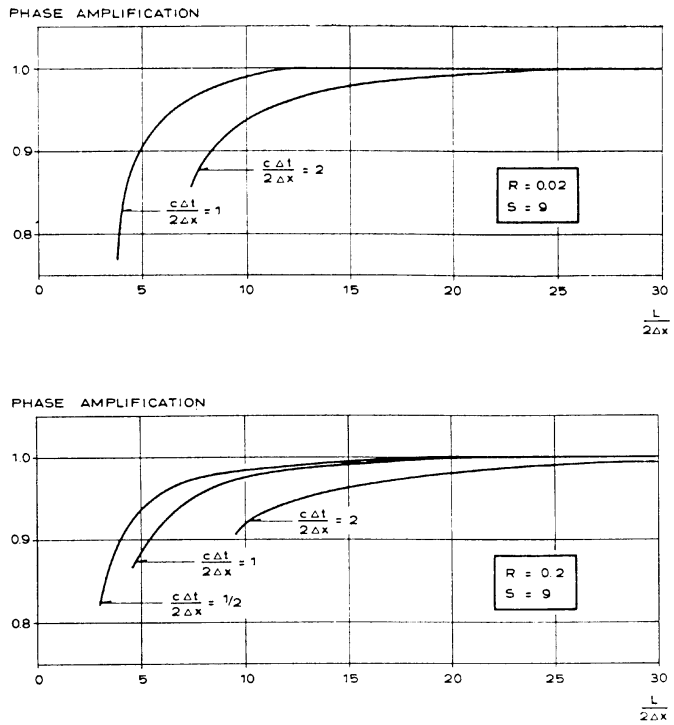

Experimental phase representation or"portrait" of the performance envelope, based upon test runs with the System in a onr-dimensional mode.

Fig. 4. Représentation de phase expérimentale (ou „portrait") de l'enveloppe des caractéristiques, obtenue à partir des résultats déterminés en exploitant le Système en mode uni-dimensionnel.

One-dimensional tests were also made for partial reflections using a generalisation of the SOMMERFELD boundary module of the Mark 6. Some results are shown in Fig. 5. Although these were generally very successful, the field test described below indicated that the physical mechanism of reflection and transmission could be introduced into the system so accurately that the SOMMERFELD boundary module could be relegated to external boundaries of the model domain.

Whereas a great deal of reference material was available for one-dimensional testing, very little material was available for two dimensional testing, outside of the field testing that is described in the next section. Comparisons were, however, made with the classical SOMMERFELD diffraction (1896) solution of linearised wave theory, by running a system-built model with waves of very small amplitude, to give the results shown in Fig. 6a. Once again, the agreement between the present general method run so restrictively and the necessarily restricted linearised theory is seen to be very satisfactory. Fig. 6b shows a perspective plot of the situation shown in plan in Fig. 6a, whereby the partial standing waves, especially, appear in a visually familiar form.

Comparisons with physical experiments

After the method had been tested over the whole operational range of wave heights and lengths shown in Fig. 4, tests were made on shoaling waves comparing computed results with the experimental results reported by MADSEN and MEI [1969]. Some typical results are shown in Fig. 7.

a.

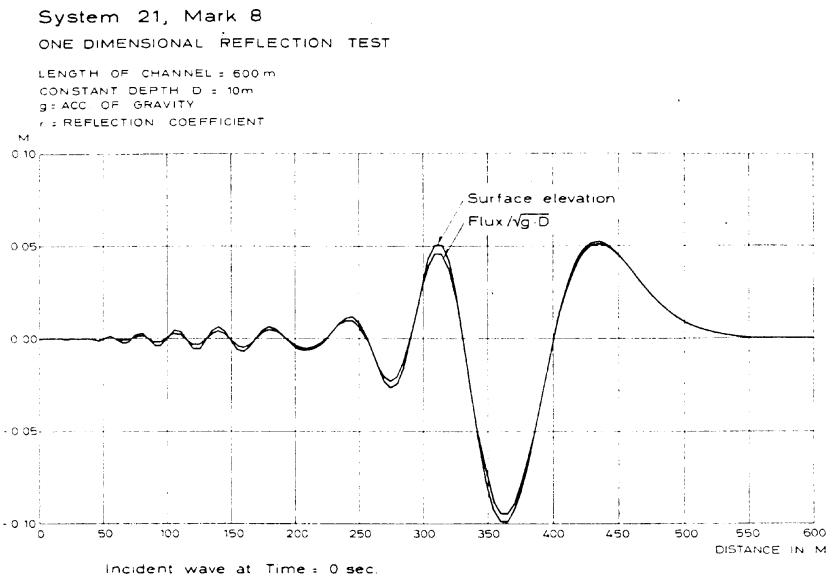

Test of total, zero and partial wave energy reflections obtained using the SOMMERFELD boundary module.

Fig. 5.

Résultats d'une étude des réflexions totale, nulle et partielle de l'énergie de l'onde, déterminées au moyen du module pariétal de SOMMERFELD.

b.

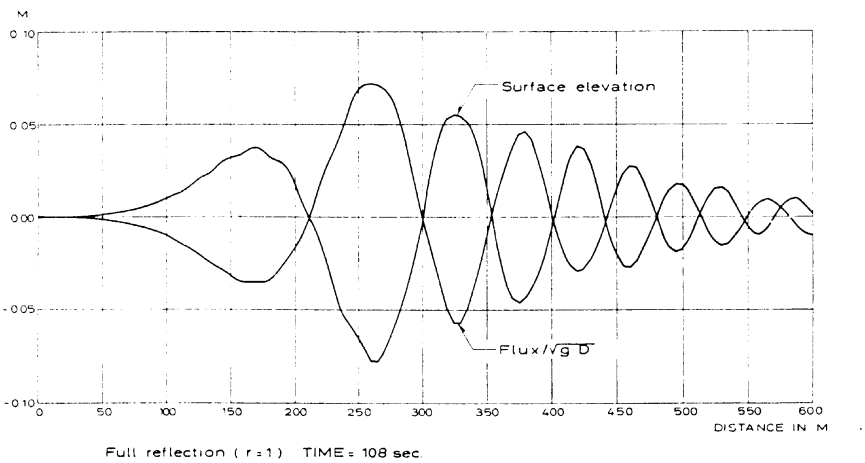

c.

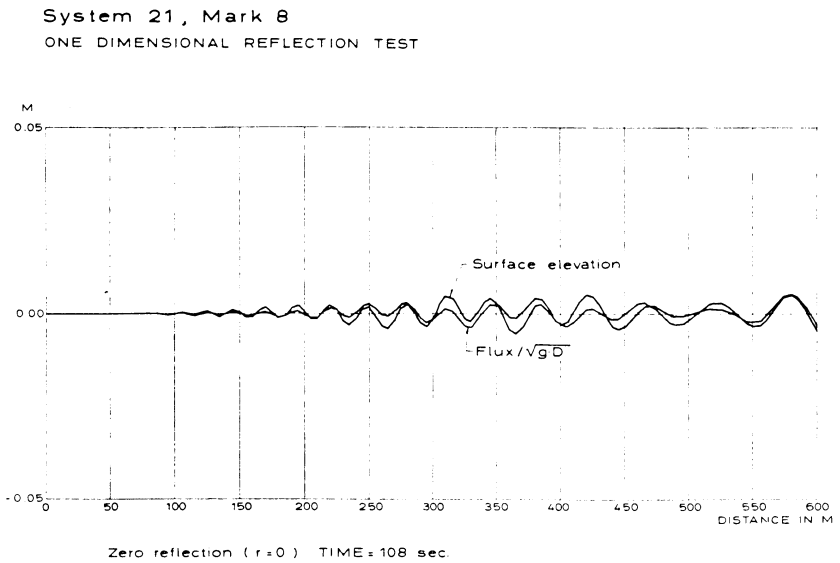
System 21, Mark 8
ONE DIMENSIONAL REFLECTION TEST
M
0.05
0.00
-0.05
Surface elevation
Flux/√g D
0
50
100
150
200
250
300
350
400
450
500
550
600
DISTANCE IN M
Zero reflection (r = 0) TIME = 108 sec.

Fig. 5.

d.

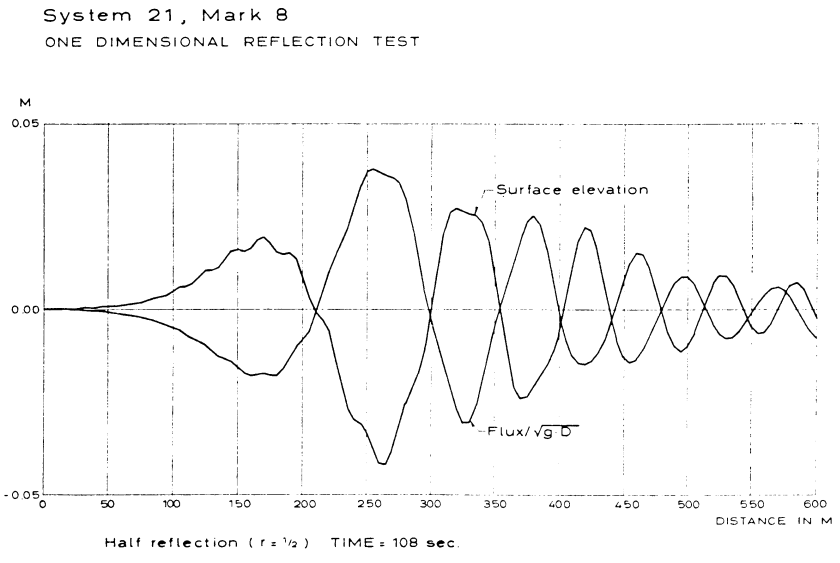
System 21, Mark 8
ONE DIMENSIONAL REFLECTION TEST
M
0.05
0.00
-0.05
Surface elevation
Flux/√g D
0
50
100
150
200
250
300
350
400
450
500
550
600
DISTANCE IN M
Half reflection (r = ½) TIME = 108 sec.

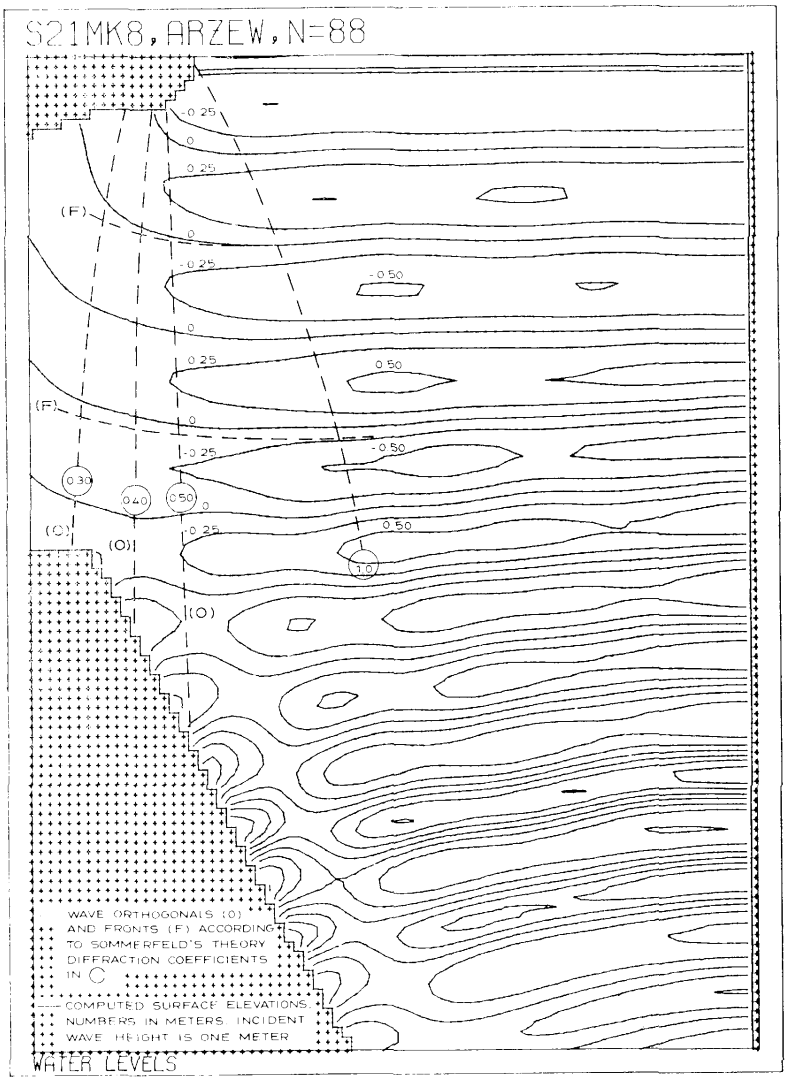

Fig. 6. Comparison of two-dimensional computations of pure diffraction with the analytical results of SOMMERFELD.
a. Plan view of elevation contours;

Fig. 6. Comparaison des résultats des calculs bidimensionnels de la diffraction pure, et des résultats analytiques déterminés par SOMMERFELD.
a. Représentation en plan des „courbes de niveau"

Agreement between computed and mean measured results were maintained to within 5% in elevation, over the whole test range, which represents a higher accuracy than that to be expected in the individual physical tests themselves.

Tests were next made of reflection and transmission of waves through permeable breakwaters, using a scheme generalised to be consistent with (11, 12, 13) throughout the domain of the computation, with porosity set to its physical value in the breakwater and set to unity in the open water, so that in open water this scheme degenerates to be consistent with (4, 5, 6). Simulations were

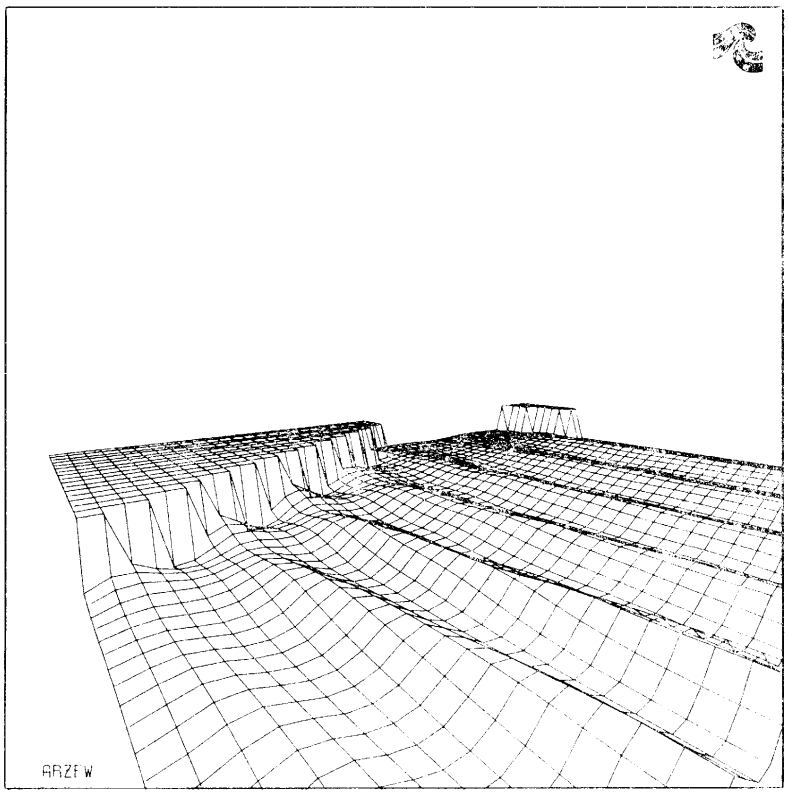

b. perspective plot of the situation shown in a.

b. Représentation en perspective de la configuration de la figure a.

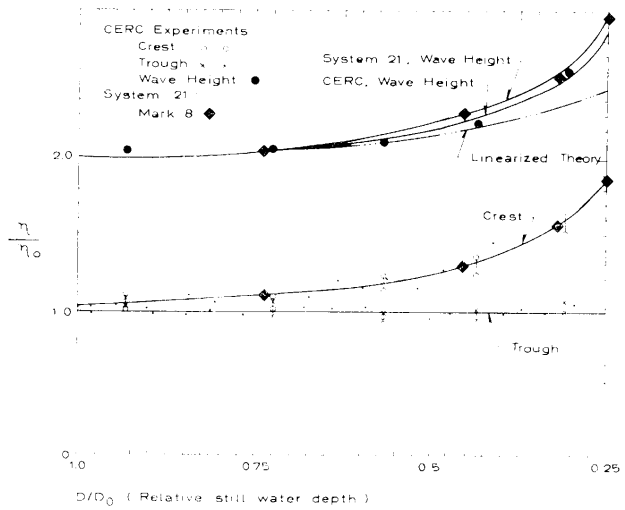

Comparison of numerical computations of shoaling waves obtained using the System in one-dimensional mode, as compared with the experimental results of MADSEN and MEI (1969).

Fig. 7.

Comparaison des résultats de calcul des ondes se propageant sur hauts-fonds, déterminés en exploitant le Système en mode uni-dimensionnel, et des résultats expérimentaux déterminés par MADSEN et MEI (1969).

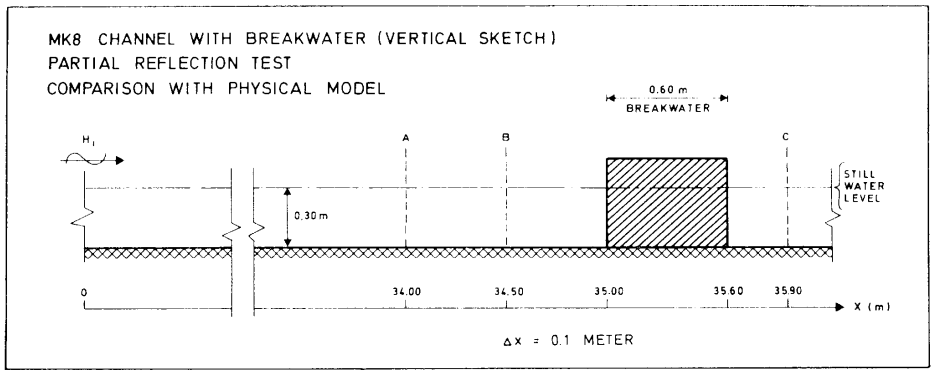

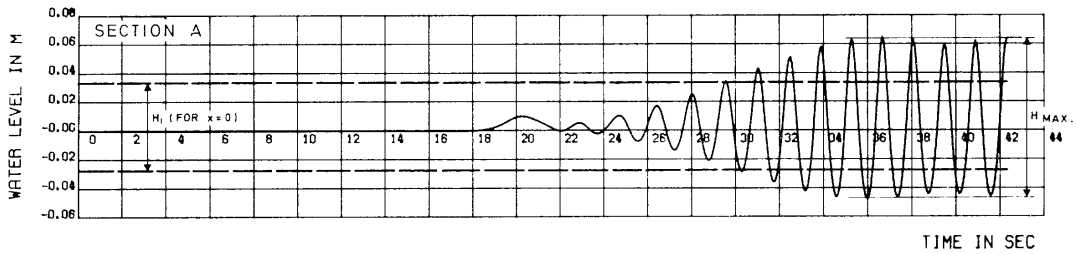

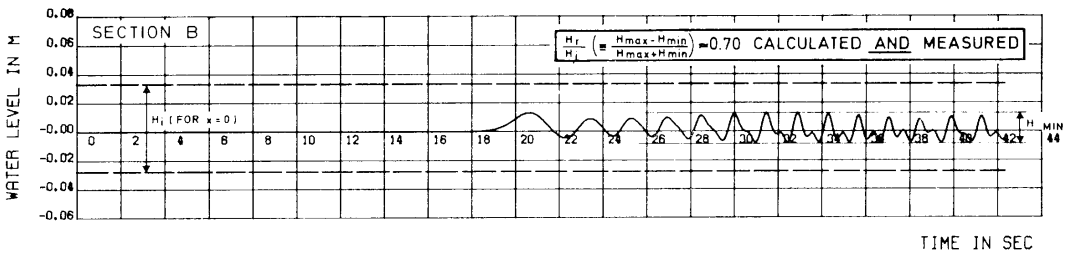

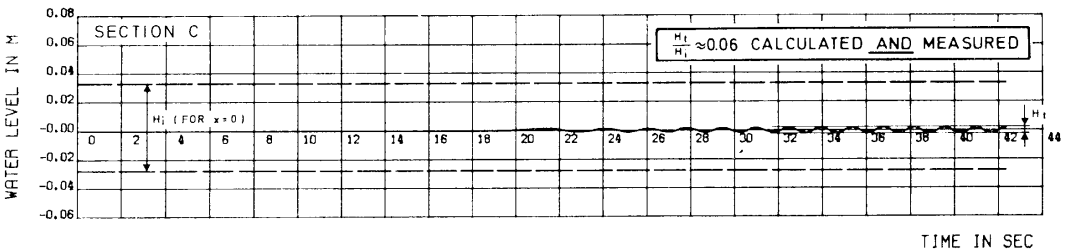

Water elevation for wave transmission through a permeable breakwater, with partial reflection, obtained using the System in one-dimensional mode. The experimental results obtained by the U.S. Army Engineer Waterways Experimental Station, Vicksburg, are used for the comparison.

Fig. 8. Surélévation du plan d'eau, correspondant à la transmission de l'onde à travers une digue perméable en présence de réflexions partielles, déterminée en exploitant le Système en mode uni-dimensionnel.
Comparaison avec les résultats expérimentaux déterminés dans les laboratoires du U.S. Army Engineers Waterways Experimental Station, Vicksburg.

a. Aerial photograph of harbour at Hanstholm.

Fig. 9.

a. Photographie aérienne du port de Hanstholm.

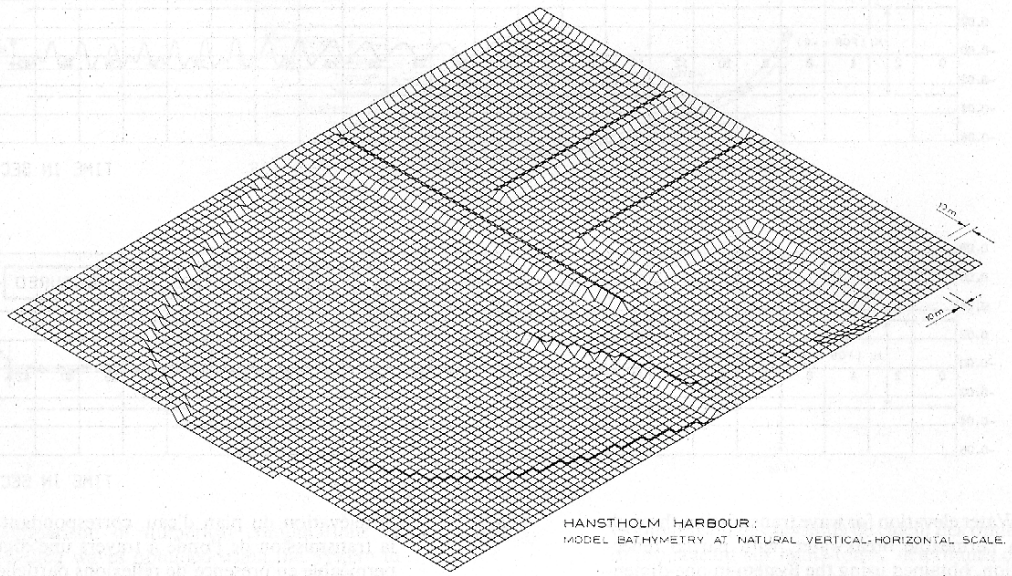

b. the numerical model bathymetry at natural vertical-horizontal scale.

b. Bathymétrie numérique, déterminée sur un modèle sans distorsion d'échelle.

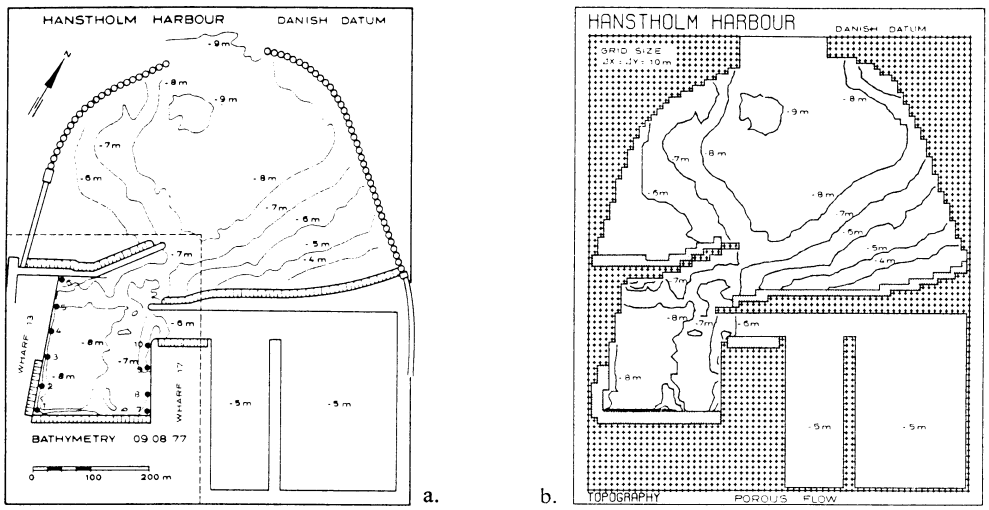

Fig. 10. Contours of the Hanstholm harbour as
a. used in the physical model tests and
b. used in the numerical model tests. The porous areas are shown in both a and b.

Courbes de niveau bathymétriques du port de Hanstholm ,prises en compte:
a. pour les essais sur modèle réduit,
b. pour les essais sur modèle numérique.

made of physical tests reported by the U.S. Army Engineer Waterways Experimental Station, Vicksburg [KEULEGAN, 1973]. As shown in Fig. 8, the agreement between the computed and experimental results is within a few percent, and again within the range of the experimental error.

With the main capabilities of the System proven, comparisons could be made between results of the system running in its full two-dimensional mode and results obtained in a physical model of a real harbour. For the purpose of comparison, the Danish harbour of Hanstholm was selected, this having been exceptionally well-documented and physical-model studied. The layout of the harbour is shown in Fig. 9, while Fig. 10a and b show the physical model bathymetry and mathematical model bathymetry respectively.

Physical model tests had been made both with periodic waves, over the full range of observed wave periods, and also with irregular (field-measured) waves. As is now well-established [e.g. SORENSEN, 1973], periodic wave tests usually give exceedingly unreliable results: small variations in incident wave period give considerable changes in amplifications of the incident wave at fixed measuring points while these amplifications can vary rapidly with the location of a measuring point. For this and other reasons, [SORENSEN, 1973], it is now standard practice to run short wave models with irregular waves, generated using irregular wave generators that are themselves programmed from field-measured time series of water surface elevations.

Comparisons between the mathematical and physical models were first made for the case of periodic wave inputs. In view of the rapid variation of amplification with distance, each measuring point in the physical model was associated with its three most closely adjacent measuring points in the mathematical model. Comparisons were made for 12 seconds and 17 second periodic waves, with the results shown in Fig. 11. It is seen that the agreement is highly satisfactory, especially when account is taken of the uncertainties in the physical model testing. By way of providing a demonstration of these uncertainties, Fig. 12a shows one of the elevation time-series plots used to obtain Fig. 11, where the variation in amplification at three immediately adjacent points is easily seen. Similarly, Fig. 12b shows the effect of merely increasing the period from the 12 seconds of

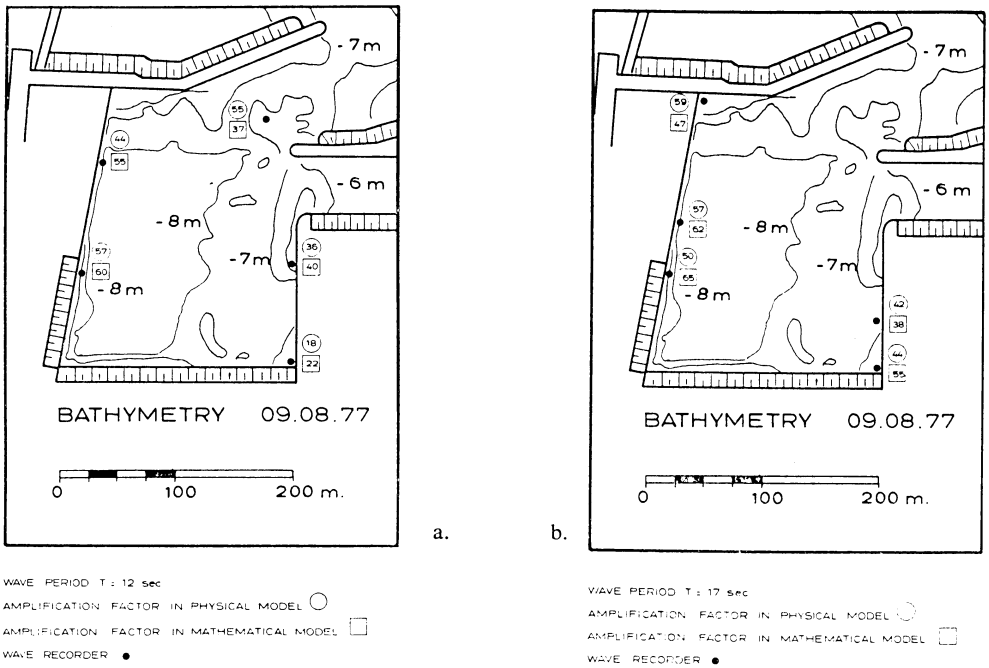

Fig. 11.

Comparisons between amplification factors obtained in the first inner harbour in the physical model with those computed using the System, for 12s and 17s periodic waves of 10 cm amplitude applied at the harbour entrance. With this small amplitude, the behaviour is almost linear.

Les zones poreuses sont réprésentées sur les deux figures.
Confrontation des coefficients d'amplification, déterminés dans le premier port intérieur sur le modèle réduit, à ceux calculés à l'aide du modèle du Système, pour des ondes incidentes de périodes 12s et 17s et d'amplitude 10 cm à l'entrée du port. Les caractéristiques correspondant à cette faible amplitude sont quasi-linéaires.

Fig. 12a to 12,5 seconds, demonstrating further the oversensivity of periodic wave testing with fixed measuring stations. Some improvements in periodic wave testing are obviously possible when using the mathematical model, as by averaging amplifications over areas of interest, but since the system – generated models run just as well with irregular waves as regular waves, there seems to be little point in refining investigation techniques along these lines. (Moreover, even these refinements would be of little help for combined mathematical and physical model testing, as envisaged for future investigations of combined ship-fendering-mooring systems).

The comparisons with irregular waves proceeded on the basis of surface elevation measurements made at the entrance to the complete harbour, so that here, as in the periodic wave tests as well, the SOMMERFELD boundary module was not activated. A typical comparison between root mean square elevations in physical and mathematical models is shown in Fig. 13. In order to provide a more visually satisfactory presentation, comparable with that obtained with a physical model, Fig. 14 shows some contour plots, separated in time by one wave period, and a perspective plot from the Hanstholm computations, for periodic waves. When running on an IBM 370/165 installation in PL/1, the Hanstholm harbour computations shown used between 1 and 1,5 second of CPU time for each 1 second of physical simulation. This time can doubtless be improved considerably by program optimisation and the use of newer machines.

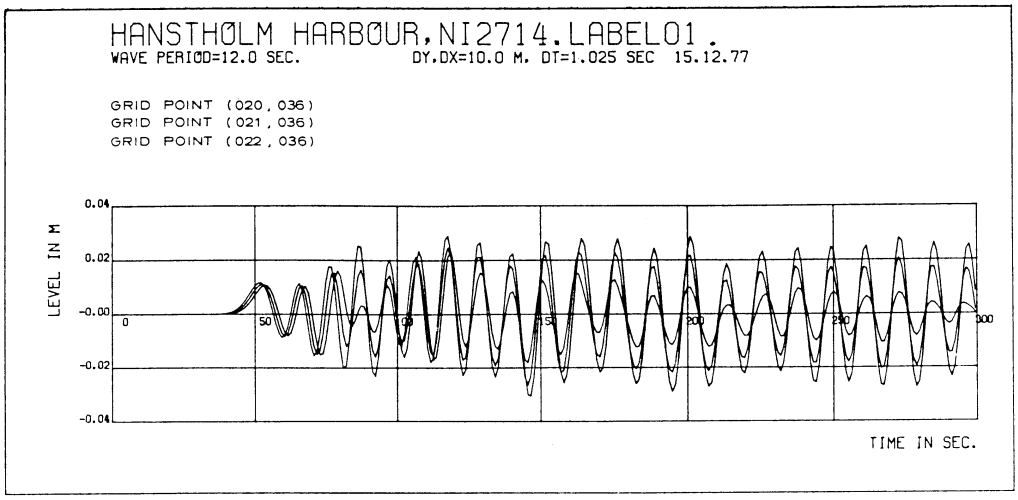

a. Time series of periodic water elevations taken at three adjacent points in the inner harbour of the numerical model, as used to generate Fig. 11, illustrating the rapid variations of elevations in space.

Fig. 12.

a. Cotes successives du plan d'eau dans le temps, relevées en trois points adjacents dans le port intérieur du modèle numérique, et utilisées pour établir la figure 11: la rapidité des variations du plan d'eau ressort très nettement de cette représentation.

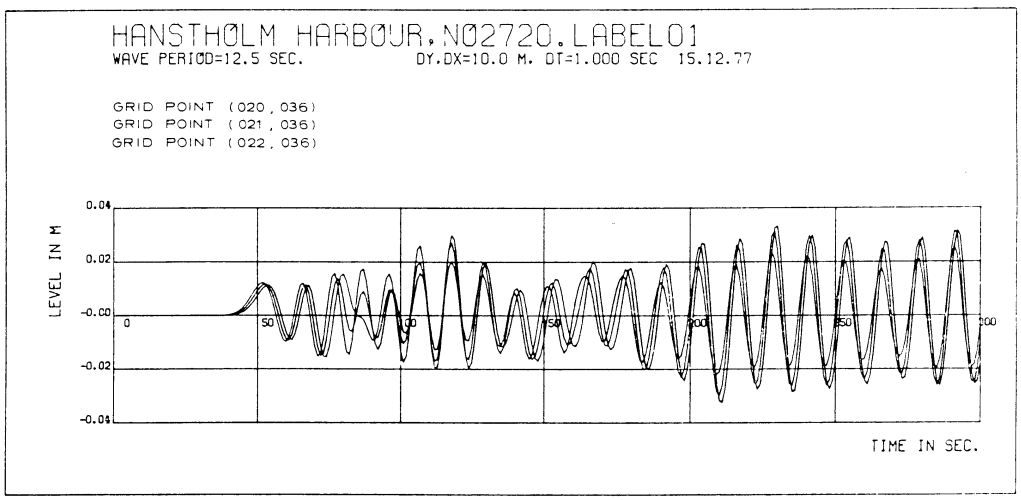

b. When the 12s period wave is replaced by a 12,5s period wave, the amplifications obtained at fixed points are seen to change considerably, a behaviour that is well-established in physical modelling.

b. Au passage de la période de 12s à 12,5s, on constate une très sensible variation des amplitudes relevées en des points fixes bien définis: il s'agit d'un phénomène bien connu sur les modèles réduits.

IRREGULAR WAVES

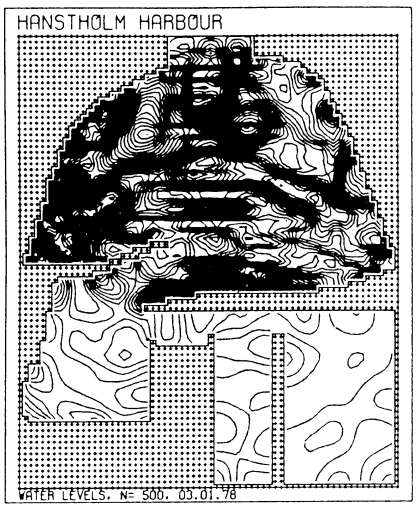

a.

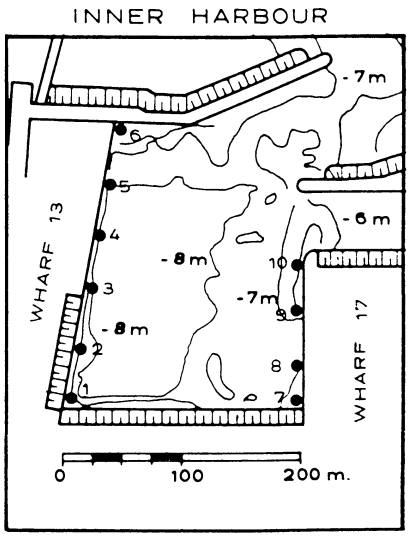

b.

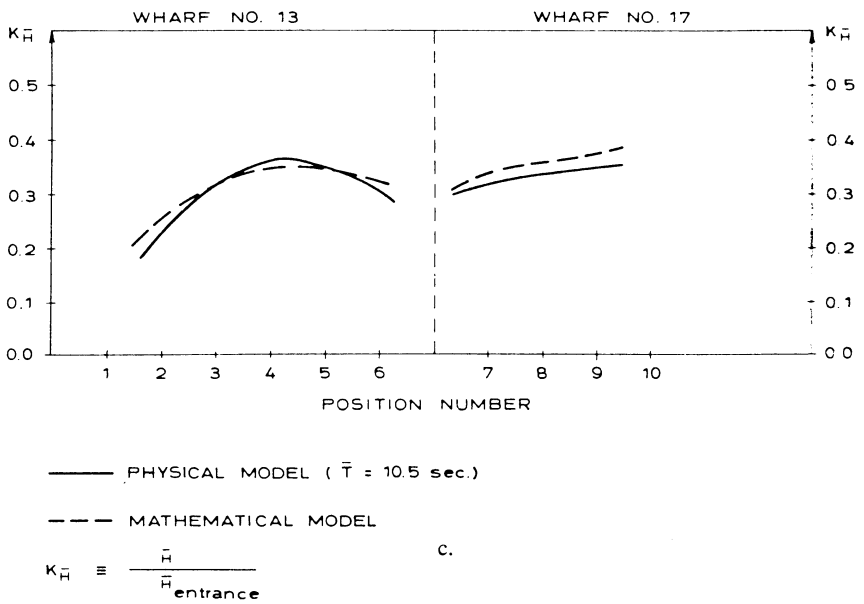

c.

a. Surface elevation contours with irregular waves (Significant wave height ≈ 1.5 m).
b. Measuring stations in the physical model.
c. Comparison between amplification factors obtained in the first inner harbour in the physical model with those computed using the System model, for tests with irregular, field-measured waves, applied at the harbour entrance.

Fig. 13.

a. „Courbes de niveau" du plan d'eau, en présence d'ondes irrégulières (amplitude significative ≈ 1,5 m).
b. Emplacements des stations de mesure sur le modèle réduits.
c. Confrontation des coefficients d'amplification, déterminés dans le premier port intérieur sur le modèle réduit, à ceux calculés à l'aide du modèle du Système, correspondant à des essais effectués avec des ondes incidentes irrégulières à l'entrée du port (déterminées à partir des résultats de mesures effectuées dans la nature).

REGULAR WAVES

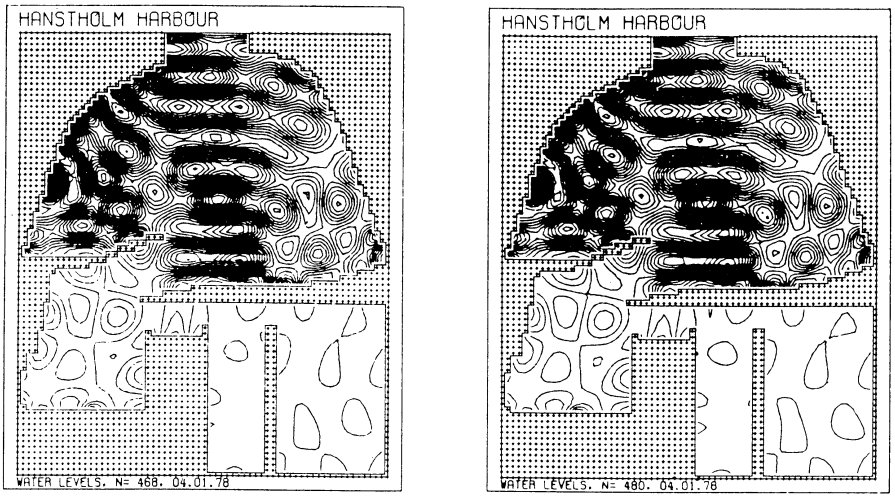

a. Surface elevation contours with regular waves compared for a one wave period time difference to illustrate the steady state attained.

Fig. 14.

a. „Courbes de niveau" du plan d'eau, en présence d'ondes régulières: comparaison pour une différence de temps correspondant à une période d'onde, destinée à mettre en évidence le régime permanent établi.

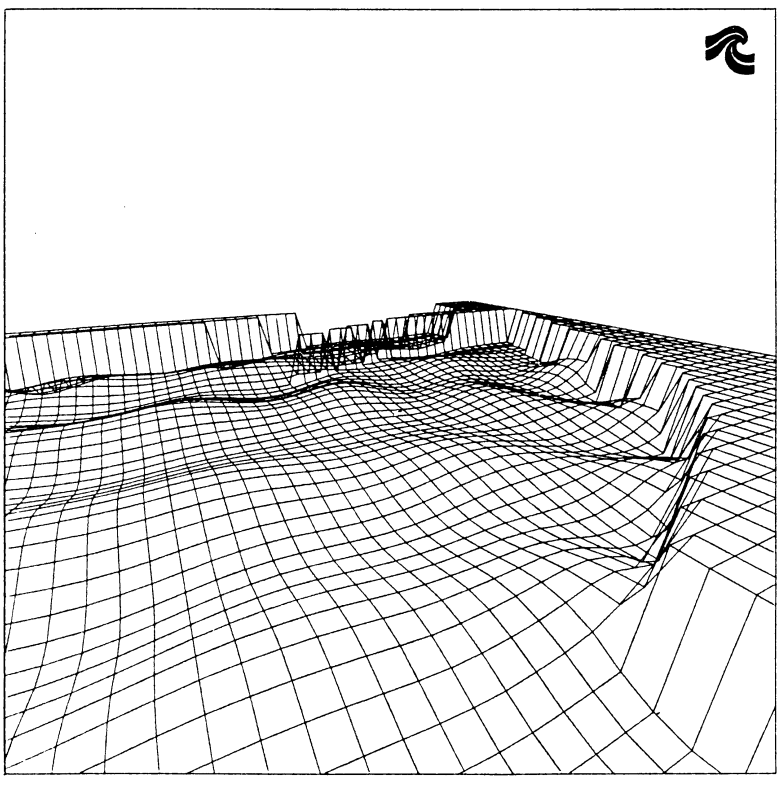

b. A perspective plot of waves in the outer harbour (view from the harbour entrance).

b. Représentation en perspective des ondes dans l'avant-port. (Vue du port de l'entrée).